Biophysical Chemistry 148 (2010) 51–55

Contents lists available at ScienceDirect

Biophysical Chemistry

journal homepage: http://www.elsevier.com/locate/biophyschem

Spectroscopic study on the binding of porphyrins to $(G_4T_4G_4)4$ parallel G-quadruplex

Chunying Wei *, Junhong Wang, Meiying Zhang

Key Laboratory of Chemical Biology and Molecular Engineering of Ministry of Education, Institute of Molecular Science, Shanxi University, Taiyuan 030006, China

ARTICLE INFO

Article history:
Received 19 December 2009
Received in revised form 19 January 2010
Accepted 10 February 2010
Available online 16 February 2010

Keywords:
Molecular crowding
G-quadruplexes
Interaction
Porphyrin
Antitumor drugs
Spectroscopy

ABSTRACT

The binding mode and stoichiometry of the cationic porphyrin TMPyP4 to G-quadruplex structure are still controversial to date, mainly due to the intricate polymorphism of G-rich sequences in the different conditions of solution. Here in the presence of the molecular crowding agent PEG, the binding interaction of TMPyP4 and another porphyrin derivative TPrPyP4 with four-stranded parallel $(G_4T_4G_4)4$ G-quadruplex was studied systematically using circular dichroism, visible absorption titration, and steady-state and time-resolved fluorescence spectroscopies. The results show that each $(G_4T_4G_4)4$ molecule is able to bind four TMPyP4 or TPrPyP4 molecules. Two types of independent and nonequivalent binding sites with the higher and lower binding affinity are confirmed, and the stronger and weaker binding constants are 2.74×10^8 and $8.21\times10^5\ M^{-1}$ for $(G_4T_4G_4)4$-TMPyP4, 2.05×10^8 and $1.05\times10^6\ M^{-1}$ for $(G_4T_4G_4)4$-TPrPyP4, respectively. The two porphyrin molecules stack on the two ends of G-quadruplex with the higher binding affinity, another two porphyrins bind weakly to the two external grooves.

1. Introduction

Guanine-rich DNA sequence $(G_4T_4G_4)$ in *Oxytricha nova* telomeric end can form an antiparallel dimer $(G_4T_4G_4)2$ G-quadruplex structure in the presence of some ions, such as Na^+, K^+ and NH_4^+ [1–3]. G-quadruplex DNAs can inhibit the activity of telomerase in cancer cell and have drawn a considerable attention by acting as a promising anticancer drug target [4–6], so understanding the mechanisms of interactions between small molecules and G-quadruplex DNAs is crucial for the design of novel anticancer drugs.

The binding of 5,10,15,20-Tetrakis(*N*-methylpyridinium-4-yl)-21*H*,23*H*-porphyrin (TMPyP4), a well-studied planar cationic porphyrin, to different types of G-quadruplex structures has been studied extensively since it can inhibit the activity of telomerase upon binding to telomeric G-quadruplex [7]. Several different models of TMPyP4 binding to quadruplexes have been proposed on the basis of structural, spectroscopic, calorimetric, or computational studies. Features of various models include the intercalative binding of the drug between two adjacent G-quartets [8–12], and/or stacking on the external G-tetrads or with the loops of the quadruplexes [8,13–17] and a weaker external binding [12,18–23]. This is further complicated by the intrinsic structural polymorphism of quadruplexes. Also the binding stoichiometry of TMPyP4 to quadruplex is not fully established.

As we know, the dimer antiparallel G-quadruplex structure formed by the $G_4T_4G_4$ sequence in *O. nova* telomere has been determined by both NMR and X-ray techniques. Interestingly, it has been shown that the conformation of this G-quadruplex is dependent on the condition of the aqueous environment, and a parallel four-stranded $(G_4T_4G_4)4$ structure was found in Na^+ and 2 M poly (ethylene glycol) (PEG 200)-containing solution [24]. In our previous study on interactions of the $d[AG_3(T_2AG_3)_3]$ sequence with TMPyP4 and TPrPyP4 (5,10,15,20-Tetrakis(N-propylpyridinium-4-yl)-21H,23H-porphyrin) in both dilute solution and crowding condition [23], the different binding mode was observed in the presence and absence of the crowding agent PEG 200, and there are different binding behaviors for TMPyP4 and TPrPyP4 molecules. Also a distinct binding behavior of TMPyP4 to the $d[AG_3(T_2AG_3)_3]$ sequence was also reported recently in both dilute solution and crowding conditions [25]. It is therefore apparent that the binding mode of porphyrins to quadruplex molecules depends on the chemical features of the porphyrin, on the structure and composition of the target DNA, and on the solution conditions in the experiment. However, all the previous studies do not take into account the binding of TMPyP4 to the parallel $(G_4T_4G_4)4$ structure in the crowding condition.

We study here the interaction of TMPyP4 (Scheme 1A) with parallel four-stranded $(G_4T_4G_4)4$ G-quadruplex under molecular crowding condition using circular dichroism (CD), visible absorption, and steady-state and time-resolved fluorescence spectroscopies, and the binding stoichiometries, association constants and binding modes of TMPyP4 with $(G_4T_4G_4)4$ G-quadruplex were first investigated in detail. To clarify the effect of the cation side arm around porphyrin core, the interaction of another porphyrin derivative, 5,10,15,20-Tetrakis(N-propylpyridinium-4-yl)-21H,23H-porphyrin (TPrPyP4)

Abbreviations: TMPyP4, 5,10,15,20-Tetrakis(*N*-methylpyridinium-4-yl)-21*H*,23*H*-porphyrin; TPrPyP4, 5,10,15,20-Tetrakis(*N*-propylpyridinium-4-yl)-21*H*,23*H*-porphyrin; CD, circular dichroism; PEG, poly(ethylene glycol).

* Corresponding author. Tel.: +86 351 7010699; fax: +86 351 7011022.
E-mail address: weichuny@sxu.edu.cn (C. Wei).

0301-4622/$ – see front matter © 2010 Elsevier B.V. All rights reserved.
doi:10.1016/j.bpc.2010.02.009

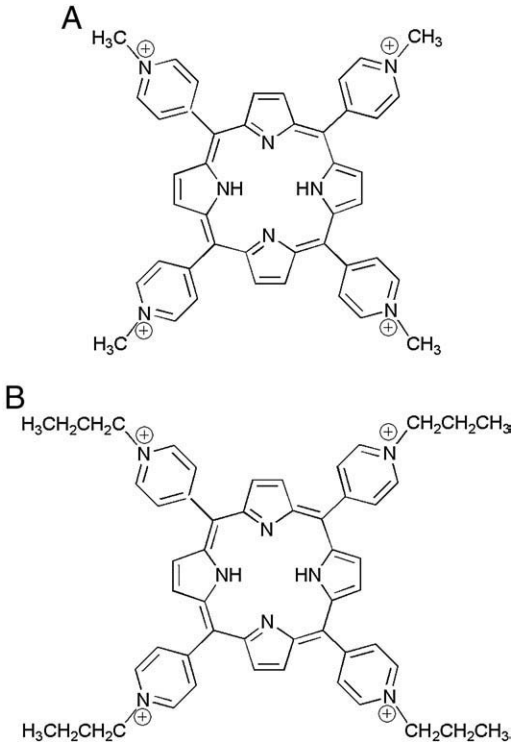

Scheme 1. The structures TMPyP4 (A) and TPrPyP4 (B).

(Scheme 1B), bearing N-propylpyridinium cationic side arms, with $(G_4T_4G_4)4$ was also studied.

2. Experimental

2.1. General

The DNA oligonucleotide $G_4T_4G_4$ was purchased from the SBS Genetech Co., Ltd. (China) in a PAGE-purified form. TMPyP4 was purchased from Sigma-Aldrich. Single-stranded concentration was determined by measuring the absorbance at 260 nm at a high temperature. Single-stranded extinction coefficient of $G_4T_4G_4$ at 260 nm is 115 200 M^{-1} cm^{-1} for [8]. The formation of G-quadruplex was carried out as follows: the oligonucleotide sample, dissolved in a buffer solution consisting of 10 mM Tris–HCl, 1 mM Na_2 EDTA, 100 mM NaCl and 40% PEG at pH 7.5, was heated to 90 °C for 5 min, gently cooled to room temperature, and then incubated at 4 °C overnight. TPrPyP4 was synthesized according to our previous published procedure [26]. The concentrations of both TMPyP4 and TPrPyP4 were determined by measuring the absorbances at 424 and 423 nm with an extinction coefficient of 2.26×10^5 and 2.1×10^5 M^{-1} cm^{-1}, respectively [8,23].

2.2. Absorption spectroscopy

Absorbance spectra were measured on a HP 8453 ChemStation with 1 cm-path-length quarter cell. Visible absorption titrations were terminated when the wavelength and intensity of the absorption band for porphyrin did not change any more upon three successive additions of G-quadruplex.

The titration data obtained were applied to construct the binding plots of r/C_f versus r using the Eq. (1) or the binding plots of r against C_f using the Eq. (2). Where r is the moles of porphyrin bound to per mole of G-quadruplex, n is the numbers of equivalent binding sites, and K is the affinities of ligands for those sites [8,27], C_f is the concentration of free porphyrin, and further details were given in the literatures [8,23]. Nonlinear regression analysis of the data was performed in the software of Origin 7.0 and errors were given as standard deviation obtained from the fits.

$$\frac{r}{C_f} = nK - Kr \tag{1}$$

$$r = \frac{n_1 K_1 C_f}{1 + K_1 C_f} + \frac{n_2 K_2 C_f}{1 + K_2 C_f} \tag{2}$$

The percent hypochromicities of the Soret bands of porphyrins can be calculated using hypochromicity $\% = [(\varepsilon_f - \varepsilon_b)/\varepsilon_f]\times 100$, where $\varepsilon_b = A_b/C_b$ [23].

2.3. CD spectroscopy

CD experiments were performed at room temperature using MOS-450/AF CD spectropolarimeter (Bio-Logic, France). Each measurement was the average of five repeated scans recorded from 220 to 320 nm in a 1 cm-path length quartz cell at a scanning rate of 50 nm/min. The concentration of G-quadruplex is 5 μM. The scan of the buffer alone was subtracted from the average scan for each sample.

2.4. Steady-state and time-resolved fluorescence spectroscopies

Steady-state fluorescence measurements were performed using Varian Cary Eclipse fluorescence spectrophotometer, excitation wavelength is set at 430 nm, and the slit width is 5 nm for both excitation and emission. Time-resolved fluorescence measurements were performed using FL920 lifetime fluorescence spectrometer (Edinburgh Instruments, UK) operating in the time-correlated single photon counting (TCSPC) mode. The samples were excited by 405.6 nm picosecond pulsed diode laser with pulse width 64.2 ps for time-resolved fluorescence measurement. All decay traces were measured using 4096-channel analyzer. The time resolution per channel was 24 ps. The number of peak counts was approximately 7000. For data analysis commercial software by Edinburgh Instruments was used. The data were fitted using a reconvolution method of the instrument response function (IRF) producing χ^2 fitting values of 1–1.3, and errors were given as standard deviation obtained from the fits. All these measurements were carried out three times to check the reproducibility and to obtain the average values for the lifetimes.

3. Results and discussion

3.1. Structural characterization of G-quadruplex

CD spectroscopy was carried out to characterize the exact structure of $G_4T_4G_4$ in Na^+ buffer containing 40% PEG (Fig. S1), and its CD spectrum shows a positive peak at 263 and a weak negative peak near 240 nm, suggesting that a parallel G-quadruplex is formed, which is consistent with the reported structure previously [24].

3.2. Binding stoichiometries and binding constants of porphyrins to G-quadruplex

The binding behaviors of both TMPyP4 and TPrPyP4 to $(G_4T_4G_4)4$ G-quadruplex were first investigated using the visible absorption titration spectra of porphyrins by addition of different concentrations of G-quadruplex (Fig. 1A,B). The result shows a 11 nm red shift at the Soret bands of both TMPyP4 and TPrPyP4 at the end of titration, whereas their hypochromicities are 61 and 59% for TMPyP4 and TPrPyP4, repectively.

Furthermore, the change of the maximum absorbance (424 and 426 nm) in the absorption spectra of TMPyP4 and TPrPyP4 was used to construct Scatchard plots using Eq. (1). Scatchard plots obtained are all nonlinear and upwardly concave (Fig. S2), which suggests that there are more than one type of binding site for TMPyP4 and TPrPyP4

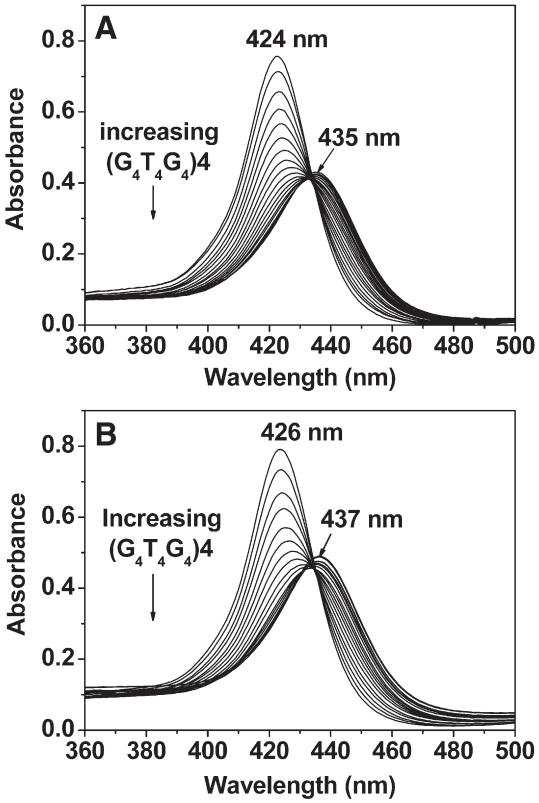

Fig. 1. Absorption titration of 3.5 μM TMPyP4 (A) or TPrPyP4 (B) with $(G_4T_4G_4)4$ G-quadruplex in the presence of 100 mM NaCl and 40% PEG. All spectra were measured in 10 mM Tris–HCl (pH 7.5) and 1 mM Na_2EDTA buffer solution.

in G-quadruplex, or that there are neighbor exclusion effects between two ligands. Scatchard plots are linear only for ligands binding to independent and equivalent sites [28].

To clarify whether curvature in Scatchard plot is due to two types of binding sites or to neighbor exclusion effects, data are analyzed using Eq. (2) and the fit results are summarized in Table 1. The good fit results obtained by Eq. (2) (Fig. S3) indicate that there are two types of binding sites, and one binding does not influence the binding on another site.

According to the fitting results, the binding constants for first (K_1) and second site (K_2) of TMPyP4 to $(G_4T_4G_4)4$ are 2.74×10^8 and $8.21\times10^5\ M^{-1}$ respectively, whereas the binding affinities for first (K_1) and second site (K_2) are 2.55×10^8 and $1.05\times10^6\ M^{-1}$ for TPrPyP4, respectively. The binding stoichiometries are 2.07 and 1.89 for the first interaction, while they are 1.98 and 1.81 for the second binding in the case of $(G_4T_4G_4)4$-TMPyP4 and $(G_4T_4G_4)4$-TPrPyP4 complexes. Thus the stoichiometry of both porphyrins for the first and second binding site is 2. Interestingly, a low-affinity binding mode was also detected at stoichiometry greater than 1 for human telomeric $AG_3(T_2AG_3)_3$ or $(TG_4T)4$ [13,18,25,26].

The binding affinities of both TMPyP4 and TPrPyP4 to site 1 (K_1) are about two orders of magnitude larger than those to site 2 (K_2) for $(G_4T_4G_4)4$ G-quadruplex. This is consistent with the previous reports wherein porphyrin binding was indicated to present one secondary site with lower affinity [19,20]. In addition, the binding constants of some derivatives of porphyrin to *c-myc*, *c-kit* and telomeric G-quadruplexes have been determined, indicating that there are one higher and one lower affinity sites [18,21–23].

Obviously, in the presence of PEG the binding behaviors of both porphyrins to $(G_4T_4G_4)4$ are similar, and the size of side arms around porphyrin core fails to affect their binding stoichiometry and affinity. The current result about the binding stoichiometry of TMPyP4 to $(G_4T_4G_4)4$ is also consistent with our previous result in only Na^+-containing buffer [8], in which the binding stoichiometry of TMPyP4 to antiparallel dimer $(G_4T_4G_4)2$ is also 4. However, the binding stoichiometry of TPrPyP4 to antiparallel dimer $(G_4T_4G_4)2$ is 2 in only Na^+-containing buffer [26], which is different from the current result under the molecular crowding condition. This comparison revealed that the binding mode of TPrPyP4 for G-quadruplex depends on the structure of G-quadruplex and on the solution condition. Similarly, in our previous study on the binding mode of TPrPyP4 for $AG_3(T_2AG_3)_3$ [23], PEG induces the transition of $AG_3(T_2AG_3)_3$ from the hybrid structure to the parallel one, and the different binding stoichiometries were also observed, they are 1.5 and 2.0 in the presence and absence of PEG, respectively.

In addition, the different binding behaviors between TMPyP4 and TPrPyP4 with $(G_4T_4G_4)4$ or with $(G_4T_4G_4)2$ G-quadruplexes also arise from the difference of the size of the peripheral groups around the porphyrin core. As described above, $G_4T_4G_4$ sequence presents the parallel and antiparallel G-quadeuplex structures in the presence and absence of PEG, respectively. Because the parallel structure with eight G-quartets is much longer than antiparallel structure with four G-quartets, TPrPyP4 with the larger side arm is much easier to bind to the parallel G-quadruplex with the higher binding stoichiometry. The similar result was also reported for long pieces of duplex DNA, where there are no significant binding differences for both TMPyP4 and TPrPyP4 [29]. This can further explain the reason that there are the same binding stoichiometries for TMPyP4 with the smaller side arms for both parallel and antiparallel structures due to small steric hindrance.

3.3. Binding modes of porphyrins to G-quadruplex

On the basis of the absorption titration experiment, the values of hypochromicity % of both porphyrins are in the range of an intercalative binding (>35%), whereas the red shift values are slightly smaller than those of the typical intercalation (>15 nm). In fact, the red shifts (>15 nm) and hypochromicities (>35%) given for intercalative binding modes were determined for long pieces of duplex DNA [30], where the end stacking is not significant. So the red shift value and hypochromicity along with the binding stoichiometry and binding constant suggest that porphyrins interact with G-quadruplex via stacking on G-quartet and outside binding mode.

Next the steady-state and time-resolved fluorescence spectra were used to provide further insight into the binding sites of porphyrins for G-quadruplex, which gives the more detailed information of environment around a fluorophore [31]. Due to increase of solution *viscosity* and decrease of solution polarity in the presence of 40% PEG, the emission bands of both free porphyrins are split in two peaks near 650 and 714 nm [23], upon addition of G-quadruplex at a G-quadruplex/porphyrin molar ratio of 2, the emission bands are red-shifted to 658 and 717 nm and the intensities are also decreased significantly (Fig. 2).

It was reported that the outside bindings of TMPyP4 to both poly(dAdT)poly(dAdT) and RNA result in a splitting and significant increase in the intensity of the emission spectrum of TMPyP4 [32,33]. The peak positions and ratios of $Q(0,0)$ to $Q(0,1)$ intensities are in good agreement with our present results. It is worthy of noting that the fluorescence spectra of TMPyP4 in its complexes with $[poly(dG\text{-}dC)]_2$ and $[d(TACGTA)]_2$ are close to those obtained for $[poly(dAdT)]_2$ [34], but an increasing ratio of $Q(0,0)$ to $Q(0,1)$ peak intensities and red

Table 1
The binding stoichometries (n_1, n_2) and binding constants (K_1, K_2) of porphyrins to G-quadruplexes in buffer solution containing 100 mM Na^+ and 40% PEG.

Complexes	n_1	K_1 (M^{-1})	n_2	K_2 (M^{-1})
$(G_4T_4G_4)4$-TMPyP4	2.07 ± 0.03	$(2.74\pm0.05)\times10^8$	1.89 ± 0.02	$(8.21\pm0.10)\times10^5$
$(G_4T_4G_4)4$-TPrPyP4	1.98 ± 0.01	$(2.55\pm0.07)\times10^8$	1.81 ± 0.02	$(1.05\pm0.04)\times10^6$

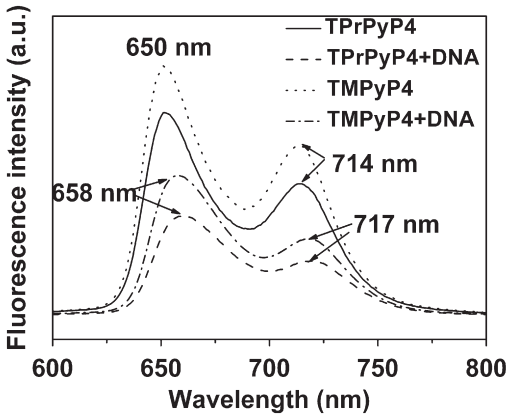

Fig. 2. Steady-state fluorescence spectra of free porphyrins and G-quadruplex-porphyrin complexes (G-quadruplex/porphyrin = 2:1) in buffer solution containing 10 mM Tris–HCl (pH 7.5), 1 mM Na_2EDTA, 100 mM NaCl and 40% PEG.

shifts of both peaks were observed in the order of $[poly(dG\text{-}dC)]_2$ < $[d(TACGTA)]_2$ < $[poly(dAdT)]_2$, which was explained by an increase of the proportion of externally bound porphyrins at the expense of intercalated ones. So these results further indicate that both porphyrins interact with G-quadruplex by outside binding and stacking on *G-quartet*.

Fig. 3 shows the fluorescence decays of porphyrins in the free form and complexes at 2:1 molar ratio of G-quadruplex to porphyrin, and their lifetime values are summarized in Table 2. For free TMPyP4 and TPrPyP4 the fluorescence decays are monoexponential, however the fluorescence decays for their complexes are biexponential, which can be explained by two different localizations of the porphyrin molecules within the G-quadruplex DNA. Two lifetimes of porphyrins further support the existence of two types of binding sites obtained by absorption titration fit.

It was reported that the lifetime of the binding TMPyP4 molecule in duplex DNA is about 10 and 1.5 ns [35–38], but assignment of both lifetimes to the intercalated or to the externally bound porphyrin is inconsistent. Generally, the longer lifetime is the externally bound porphyrin, and the shorter lifetime is the intercalated porphyrin [36,38]. In addition, in the case of TMPyP4-$[poly(dGdC)]_2$ complex, the decay kinetics is found to be biexponential and the lifetimes are 2.5 and 7.0 ns, which are markedly shorter than those of the complexes with $[poly(dAdT)_2$ (12 ns) [38]. It was found that the most probable types of interactions of porphyrin with $[poly(dGdC)]_2$ and with $[poly(dAdT)]_2$ are the stacking on base pair (containing intercalation and end stacking) and external binding, respectively. For TMPyP4-$[poly(dGdC)]_2$ complex the shorter lifetime of 2.5 ns is attributed to the intercalative porphyrin because of G base quenches

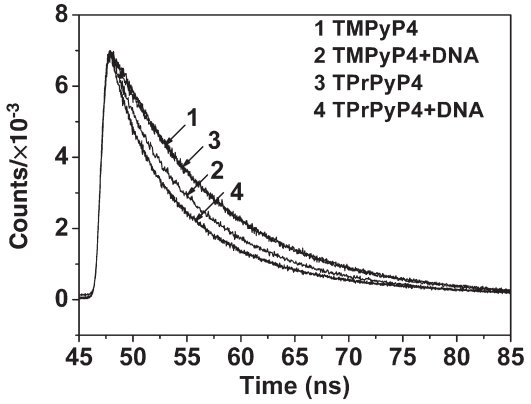

Fig. 3. Fluorescence decay curves of free porphyrins and G-quadruplex-porphyrin complexes (G-quadruplex/porphyrin = 2:1) in buffer solution containing 10 mM Tris–HCl (pH 7.5), 1 mM Na_2EDTA, 100 mM NaCl and 40% PEG.

Table 2
The fluorescence lifetimes of porphyrins in the presence or absence of G-quadruplex in buffer solution containing 100 mM Na^+ and 40% PEG.

Compounds	τ_1 (ns)[a]	τ_2 (ns)[a]
TMPyP4	10.72 ± 0.03	0
$(G_4T_4G_4)$4-TMPyP4	6.50 ± 0.01 (18.31 ± 0.12%)	10.43 ± 0.02 (81.69 ± 0.25%)
TPrPyP4	10.68 ± 0.05	0
$(G_4T_4G_4)$4-TPrPyP4	5.83 ± 0.05 (24.30 ± 0.13%)	10.23 ± 0.03 (75.70 ± 0.23%)

[a] τ values denote the fluorescence lifetimes that were obtained at 650 nm for free TMPyP4 and TPrPyP4, 658 for complexes of $(G_4T_4G_4)$4-TMPyP4 and $(G_4T_4G_4)$4-TPrPyP4, respectively. The data in bracket are the respective fractional amplitudes.

the fluorescence of porphyrin, whereas the longer lifetime of 7.0 ns is due to the porphyrin by the end-stacking binding [38]. Take these results into account, we identify the shorter lifetimes about 6 ns as belonging to the end-stacking species and the longer lifetimes about 10 ns as belonging to externally bound porphyrin molecules in the grooves.

According to the binding type, binding stoichiometry, binding affinity and fluorescence lifetime of porphyrins, we conclude that the two porphyrin molecules are stacked at the two ends of parallel $(G_4T_4G_4)$4 G-quadruplex with the stronger binding affinity, another two molecules are bound to the two grooves of $(G_4T_4G_4)$4 G-quadruplex with the weak binding affinity.

4. Conclusions

In summary, under molecular crowding conditions two types of independent and nonequivalent binding sites for both TMPyP4 and TPrPyP4 to tetramer parallel $(G_4T_4G_4)$4 G-quadruplex were confirmed, and the stronger and weaker binding affinities are 2.74×10^8 and 8.21×10^5 M^{-1} for $(G_4T_4G_4)$4-TMPyP4, 2.55×10^8 and 1.05×10^6 M^{-1} for $(G_4T_4G_4)$4-TPrPyP4, respectively. The two porphyrin molecules (TMPyP4 or TPrPyP4) stacks on the two opposite ends of parallel G-quadruplex with the stronger binding affinity, another two molecules bind to the two external grooves by the weaker binding interaction.

Acknowledgements

This work was supported by the National Natural Science Foundation of China (20673110), the Scientific Research Foundation for the Returned Overseas Chinese Scholars of Shanxi Province (2007), the Natural Science Fund of the Shanxi Province (2009011012-2), the Selected Support Foundation for the Returned Overseas Chinese Scholars of Shanxi Province (2009) and Open Foundation of Key Laboratory (N-05-05).

Appendix A. Supplementary data

Supplementary data associated with this article can be found, in the online version, at doi:10.1016/j.bpc.2010.02.009.

References

[1] S. Neidle, G.N. Parkinson, The structure of telomeric DNA, Curr. Opin. Struct. Biol. 13 (2003) 275–283.
[2] M.A. Keniry, Quadruplex structures in nucleic acid, Biopolymers 56 (2001) 123–146.
[3] P. Schultze, N.V. Hud, F.W. Smith, J. Feigon, The effect of sodium, potassium and ammonium ions on the conformation of the dimeric quadruplex formed by the *Oxytricha nova* telomere repeat oligonucleotide $d(G_4T_4G_4)$, Nucleic Acids Res. 27 (1999) 3018–3028.
[4] W.D. Wilson, H. Sugiyama, First international meeting on quadruplex DNA, ACS Chem. Biol. 9 (2007) 589–594.
[5] E.M. Rezler, D.J. Bearss, L.H. Hurley, Telomeres and telomerase as drug targets, Curr. Opin. Pharmacol. 2 (2002) 415–423.
[6] L. Oganesian, T.M. Bryan, Physiological relevance of telomeric G-quadruplex formation: a potential drug target, BioEssays 29 (2007) 155–167.
[7] E. Izbicka, R.T. Wheelhouse, E. Raymond, K.K. Davidson, R.A. Lawrence, D. Sun, B.E. Windle, L.H. Hurley, D.D. Von Hoff, Effects of cationic porphyrins as G-quadruplex interactive agents in human tumor cells, Cancer Res. 59 (1999) 639–644.

[8] C. Wei, G. Jia, J. Yuan, Z. Feng, C. Li, A spectroscopic study on the interactions of porphyrin with G-quadruplex DNAs, Biochemistry 45 (2006) 6681–6691.
[9] N.V. Anantha, M. Azam, R.D. Sheardy, Porphyrin binding to quadrupled T4G4, Biochemistry 37 (1998) 2709–2714.
[10] M. Cavallari, A. Garbesi, R.D. Felice, Porphyrin intercalation in G4-DNA quadruplexes by molecular dynamics simulations, J. Phys. Chem. B 113 (2009) 13 152–13 160.
[11] I. Haq, J.O. Trent, B.Z. Chowdhry, T.C. Jenkins, Intercalative G-tetraplex stabilization of telomeric DNA by a cationic porphyrin, J. Am. Chem. Soc. 121 (1999) 1768–1779.
[12] I. Lubitz, N. Borovok, A. Kotlyar, Interaction of monomolecular G4-DNA nanowires with TMPyP: evidence for intercalation, Biochemistry 46 (2007) 12 925–12 929.
[13] R.T. Wheelhouse, D. Sun, H. Han, F.X. Han, L.H. Hurley, Cationic porphyrins as telomerase inhibitors: the interaction of tetra-(*N*-methyl-4-pyridyl)porphine with quadruplex DNA, J. Am. Chem. Soc. 120 (1998) 3261–3262.
[14] F.X. Han, R.T. Wheelhouse, L.H. Hurley, Interactions of TMPyP4 and TMPyP2 with quadruplex DNA. Structural basis for the differential effects on telomerase inhibition, J. Am. Chem. Soc. 121 (1999) 3561–3570.
[15] H. Han, D.R. Langley, A. Rangan, L.H. Hurley, Selective interactions of cationic porphyrins with G-quadruplex structures, J. Am. Chem. Soc. 123 (2001) 8902–8913.
[16] G.N. Parkinson, R. Ghosh, S. Neidle, Structural basis for binding of porphyrin to human telomeres, Biochemistry 46 (2007) 2390–2397.
[17] G. Jia, Z. Feng, C. Wei, J. Zhou, X. Wang, C. Li, Dynamic insight into the interaction between porphyrin and G-quadruplex DNAs: time-resolved fluorescence anisotropy study, J. Phys. Chem. B 113 (2009) 16 237–16 245.
[18] A. Arora, S. Maiti, Effect of loop orientation on quadruplex-TMPyP4 interaction, J. Phys. Chem. B 112 (2008) 8151–8159.
[19] J. Seenisamy, S. Bashyam, V. Gokhale, H. Vankayalapati, D. Sun, A. Siddiqui-Jain, N. Streiner, K. Shin-ya, E. White, W.D. Wilson, L.H. Hurley, Design and synthesis of an expanded porphyrin that has selectivity for the c-MYC G-quadruplex structure, J. Am. Chem. Soc. 127 (2005) 2944–2959.
[20] T. Yamashita, T. Uno, Y. Ishikawa, Stabilization of guanine quadruplex DNA by the binding of porphyrins with cationic side arms, Bioorg. Med. Chem. 13 (2005) 2423–2430.
[21] K. Halder, S. Chowdhury, Quadruplex-coupled kinetics distinguishes ligand binding between G4 DNA motifs, Biochemistry 46 (2007) 14 762–14 770.
[22] I.M. Dixon, F. Lopez, A.M. Tejera, J.-P. Estève, M.A. Blasco, G. Pratviel, B. Meunier, G-quadruplex ligand with 10000-fold selectivity over duplex DNA, J. Am. Chem. Soc. 129 (2007) 1502–1503.
[23] C. Wei, G. Jia, J. Zhou, G. Han, C. Li, Evidence for the binding mode of porphyrins with G-quadruplex DNA, Phys. Chem. Chem. Phys. 11 (2009) 4025–4032.
[24] D. Miyoshi, A. Nakao, N. Sugimoto, Molecular crowding regulates the structural switch of the DNA G-Quadruplex, Biochemistry 41 (2002) 15 017–15 024.
[25] L. Martino, B. Pagano, I. Fotticchia, S. Neidle, C. Giancola, Shedding light on the interaction between TMPyP4 and human telomeric quadruplexes, J. Phys. Chem. B 113 (2009) 14 779–14 786.
[26] C. Wei, G. Han, G. Jia, J. Zhou, C. Li, Study on the interaction of porphyrin with G-quadruplex DNAs, Biophys. Chem. 137 (2008) 19–23.
[27] J.B. Chaires, Analysis and interpretation of ligand-DNA binding isotherms, Methods Enzymol. 340 (2001) 3–22.
[28] J.D. McGhee, P.H. von Hippel, Theoretical aspects of DNA-protein interactions: co-operative and non-co-operative binding of large ligands to a one-dimensional homogeneous lattice, J. Mol. Biol. 86 (1974) 469–489.
[29] T.A. Gray, K.T. Yue, L.G. Marzilli, Effect of N-Alkyl substituents on the DNA binding properties of meso-tetrakis(4-N-alkylpyridium-4-yl) porphyrins and their nickel derivatives, J. Inorg. Biochem. 41 (1991) 205–219.
[30] R.F. Pasternack, E.J. Gibbs, J.J. Villafranca, Interactions of porphyrins with nucleic acids, Biochemistry 22 (1983) 2406–2414.
[31] T. Lenz, E.Y.M. Bonnist, G. Pljevaljčić, R.K. Neely, D.T.F. Dryden, A.J. Scheidig, A.C. Jones, E. Weinhold, 2-Aminopurine flipped into the active site of the adenine-specific DNA methyltransferase M.TaqI: crystal structures and time-resolved fluorescence, J. Am. Chem. Soc. 129 (2007) 6240–6248.
[32] A.A. Ghazaryan, Y.B. Dalyan, S.G. Haroutiunian, A. Tikhomirova, N. Taulier, J.W. Wells, T.V. Chalikian, Thermodynamics of interactions of water-soluble porphyrins with RNA duplexes, J. Am. Chem. Soc. 128 (2006) 1914–1921.
[33] J.M. Kelly, M.J. Murphy, D.J. Mcconnell, C.A. Ohuigin, A comparative study of the interaction of 5, 10, 15, 20-tetrakis (N-methylpyridinium-4-yl)porphyrin and its zinc complex with DNA using fluorescence spectroscopy and topoisomerisation, Nucleic Acids Res. 13 (1985) 167–184.
[34] N.N. Kruk, S.I. Shishporenok, A.A. Korotky, V.A. Galievsky, V.S. Chirvony, P.-Y. Turpin, Binding of the cationic 5, 10, 15, 20-tetrakis(4-N-methylpyridyl) porphyrin at 5′CG3′ and 5′GC3′ sequences of hexadeoxyribonucleotides: triplettriplet transient absorption, steady-state and time-resolved fluorescence and resonance Raman studies, J. Photochem. Photobiol. B: Biol. 45 (1998) 67–74.
[35] Y. Shen, P. Myslinski, T. Treszczanovicz, Y. Liu, J.A. Koningstein, Picosecond laser-induced fluorescence polarization studies of mitoxantrone and tetrakis porphine/DNA complexes, J. Phys. Chem. 96 (1992) 7782–7787.
[36] K. Zupán, L. Herényi, K. Tóth, Z. Majer, G. Csík, Binding of cationic porphyrin to isolated and encapsidated viral DNA analyzed by comprehensive spectroscopic methods, Biochemistry 43 (2004) 9151–9159.
[37] Y. Liu, J.A. Koningstein, Y. Yevdokimov, Relative cross section and time-resolved fluorescence of porphyrin–DNA complexes, Can. J. Chem. 69 (1991) 1791–1803.
[38] V.S. Chirvony, V.A. Galievsky, N.N. Kruk, B.M. Dzhagarov, P.-Y. Turpin, Photophysics of cationic 5, 10, 15, 20-tetrakis-(4-N-methylpyridyl) porphyrin bound to DNA, [poly (dA-dT)]2 and [poly(dG-dC)]2: on a possible charge transfer process between guanine and porphyrin in its excited singlet state, J. Photochem. Photobiol. B: Biol. 40 (1997) 154–162.